

Research Article: New Research | Sensory and Motor Systems

Synaptic basis for contrast-dependent shifts in functional identity in mouse V1

Molis Yunzab^{1,2}, Veronica Choi³, Hamish Meffin^{1,2}, Shaun L Cloherty^{1,2,4}, Nicholas J Priebe³ and Michael R Ibbotson^{1,2}

¹National Vision Research Institute, Australian College of Optometry, 374 Cardigan Street, Carlton, VIC 3053, Australia

²Department of Optometry and Vision Sciences, University of Melbourne, Parkville, VIC 3010, Australia

³University of Texas Austin, Centre for Learning and Memory, 100 E 24th St, Austin, TX 78712, USA

⁴Department of Physiology, Monash University, Clayton, VIC 3800, Australia

<https://doi.org/10.1523/ENEURO.0480-18.2019>

Received: 11 December 2018

Revised: 12 February 2019

Accepted: 27 February 2019

Published: 20 March 2019

M.Y., N.J.P., and M.R.I. designed research; M.Y. and V.C. performed research; M.Y., V.C., H.M., S.L.C., N.J.P., and M.R.I. analyzed data; M.Y., V.C., N.J.P., and M.R.I. wrote the paper.

Funding: Australian Research Council Centre of Excellence for Integrative Brain Function
CE140100007

;

Funding: National Health and Medical Research Council
GNT0525459

;

Funding: L.E.W. Carty Charitable Fund & Lions Foundation of Victoria

;

Funding: National Health Institutes
EY-020592

.

Conflict of Interest: The authors report no conflict of interest.

M.Y. and V.C. Equal contribution

N.J.P. and M.R.I. Equal contribution

This work was supported by the Australian Research Council Centre of Excellence for Integrative Brain Function (CE140100007), the National Health and Medical Research Council (GNT0525459), the L.E.W. Carty Charitable Fund & Lions Foundation of Victoria and the National Health Institutes (EY-020592).

Correspondence should be addressed to Michael R Ibbotson at mibbotson@nvri.org.au

Cite as: eNeuro 2019; 10.1523/ENEURO.0480-18.2019

Alerts: Sign up at www.eneuro.org/alerts to receive customized email alerts when the fully formatted version of this article is published.

Accepted manuscripts are peer-reviewed but have not been through the copyediting, formatting, or proofreading process.

Copyright © 2019 Yunzab et al.

This is an open-access article distributed under the terms of the Creative Commons Attribution 4.0 International license, which permits unrestricted use, distribution and reproduction in any medium provided that the original work is properly attributed.

Manuscript Title: Synaptic basis for contrast-dependent shifts in functional identity in mouse V1

Abbreviated Title: Contrast-dependent phase sensitivity in primary visual cortex: an intracellular study

1

2 **Authors:** Molis Yunzab^{*1,2}, Veronica Choi^{*3}, Hamish Meffin^{1,2}, Shaun L
3 Cloherty^{1,2,4}, Nicholas J Priebe^{†3}, Michael R Ibbotson^{†1,2}

4 1. National Vision Research Institute, Australian College of Optometry, 374
5 Cardigan Street, Carlton, VIC 3053, Australia.

6 2. Department of Optometry and Vision Sciences, University of Melbourne,
7 Parkville, VIC 3010, Australia.

8 3. University of Texas Austin, Centre for Learning and Memory, 100 E 24th St,
9 Austin, TX 78712, USA

10 4. Department of Physiology, Monash University, Clayton, VIC 3800, Australia

11

12 * Equal contribution

13 † Equal contribution

14

15 **Author Contributions:** MY, NP and MI designed research; MY and VC performed
16 research; MY, VC, HM, SC, NP and MI analysed data; MY, VC, NP and MI wrote
17 the paper.

18

Corresponding Author: Michael Ibbotson
National Vision Research Institute
Australian College of Optometry
374 Cardigan Street
Carlton, VIC 3053, Australia
phone: +61-3-9349-7482
email: mibbotson@nvri.org.au

19

20

Number of Figures: 8

Number of Tables: 0

Number of Multimedia: 0

Number of Words: Abstract: 190
Significance Statement: 119
Introduction: 650
Discussion: 751

21 **Acknowledgements and Funding Sources:** This work was supported by the
22 Australian Research Council Centre of Excellence for Integrative Brain Function
23 (CE140100007), the National Health and Medical Research Council
24 (GNT0525459), the L.E.W. Carty Charitable Fund & Lions Foundation of Victoria
25 and the National Health Institutes (EY-020592).

26 **Conflict of interest:** The authors report no conflict of interest.

27

28 **Abstract**

29 A central transformation that occurs within mammalian visual cortex is the change
30 from linear, polarity-sensitive responses to nonlinear, polarity-insensitive responses.
31 These neurons are classically labelled as either simple or complex, respectively,
32 on the basis of their response linearity (Skottun et al., 1991). While the
33 difference between cell classes is clear when the stimulus strength is high,
34 reducing stimulus strength diminishes the differences between the cell types and
35 causes some complex cells to respond as simple cells (Crowder et al., 2007; van
36 Kleef et al., 2010; Hietanen et al., 2013). To understand the synaptic basis for
37 this shift in behaviour we used *in vivo* whole cell recordings while systematically
38 shifting stimulus contrast. We find systematic shifts in the degree of complex cell
39 responses in mouse primary visual cortex (V1) at the subthreshold level,
40 demonstrating that synaptic inputs change in concert with the shifts in response
41 linearity and that the change in response linearity is not simply due to the
42 threshold nonlinearity. These shifts are consistent with a visual cortex model in
43 which the recurrent amplification acts as a critical component in the generation
44 of complex cell responses (Chance et al., 1999).

45

46 **Significance statement**

47 The discovery of simple and complex cells in the primary visual cortex (V1) has
48 been fundamental to our understanding of visual processing. While both cell
49 types are orientation selective, simple cells are spatial phase sensitive while
50 complex cells are phase-invariant. Extracellular recordings have shown that the
51 responses of complex cells become phase sensitive at lower stimulus contrasts,
52 suggesting more flexibility in processing mechanisms than previously thought.
53 The mechanism by which this flexibility arises is not understood. Using *in vivo*
54 whole cell recordings, we demonstrated that the flexibility in phase sensitivity is
55 also apparent in the subthreshold responses of mouse V1 cells, suggesting that
56 the effect arises from active cortical recurrent network activity and not from
57 passive spiking threshold mechanisms.

58 **Introduction**

59 The receptive fields (RFs) of cells in the primary visual cortex (V1) are
60 classified as either simple or complex based on their spatial organisation (Hubel
61 and Wiesel, 1962; Henry, 1977). Simple cell RFs have segregated subfields that
62 respond to either brightness increments (ON) or decrements (OFF); complex
63 cells do not have clearly segregated ON and OFF subfields (Hubel and Wiesel,
64 1962; Gilbert, 1977; Henry, 1977; Hammond and Ahmed, 1985; Spitzer and
65 Hochstein, 1988; Mechler and Ringach, 2002; Priebe et al., 2004; Hietanen et al.,
66 2013). The Hubel & Wiesel hierarchical model proposed that convergent
67 synaptic inputs are responsible for these transformations in two stages (Hubel
68 and Wiesel, 1962): thalamic relay cells, displaced along an oriented axis,
69 converge on simple cells, generating orientation selectivity, then simple cells
70 converge on complex cells to provide polarity invariance.

71 The distinction between simple and complex cells is related to neuronal
72 laminar position and synaptic connectivity in some mammals (Ringach et al.,
73 2002; Martinez et al., 2005; Williams and Shapley, 2007). Simple cells are found
74 more often in cortical layers that receive thalamocortical connections, while
75 complex cells are found in layers with dense recurrent cortical connectivity. The
76 differences between simple and complex cell RFs may reflect a general process in
77 which cortical circuits generalize selectivity by amplifying inputs. While cortical
78 amplification has previously been hypothesized to increase selectivity
79 (Benyishai et al., 1995; Douglas et al., 1995; Somers et al., 1995), it is also
80 possible for it to generalize selectivity by integrating inputs with distinct RFs. We
81 examined whether simple and complex cell responses in V1 exhibited signatures
82 of this amplification.

83 One quantitative method to distinguish simple and complex cells depends
84 on the relative modulation of responses to drifting sinusoidal gratings (Skottun
85 et al., 1991). When stimulated with high-contrast drifting gratings, simple cell
86 responses modulate as the grating moves across the distinct ON and OFF
87 subfields. In contrast, complex cells respond to all phases of the drifting gratings.
88 Studies have demonstrated that the ratio (F_1/F_0) of the modulated spiking
89 component (F_1) to the unmodulated component (F_0) forms a bimodal
90 distribution, suggesting two classes of V1 neurons (Maffei and Fiorenti, 1973;
91 Movshon et al., 1978; De Valois et al., 1982; Skottun et al., 1991). While this
92 difference between cell classes is clear when the stimulus strength is high,
93 reducing stimulus strength diminishes the differences between the cell types. In
94 particular, low contrast gratings evoke modulated responses in many complex
95 cells (cat: Crowder et al., 2007; van Kleef et al., 2010; monkey: Henry and
96 Hawken, 2013; Cloherty and Ibbotson, 2015; Meffin et al., 2015).

97 The mechanism underlying this change in spiking modulation ratio is not
98 understood but there are two candidate models. The first model suggests that
99 modulations in response to low contrast stimuli emerge due to the “iceberg”
100 effect in which not all synaptic responses are converted into spikes (Carandini
101 and Ferster, 2000; Mechler and Ringach, 2002; Priebe et al., 2004). In this model
102 the subthreshold synaptic modulation ratio (V_1/V_0) should not depend on
103 contrast. Alternatively, there may be a shift in the synaptic inputs to V1 neurons
104 in which the V_1/V_0 ratio increases as the contrast decreases. A cortical model in
105 which the amplification acts to integrate inputs with distinct spatial preferences
106 predicts this specific change in synaptic input.

107 To distinguish these possibilities, we performed *in vivo* whole cell
108 recordings in mouse V1. Both the V_1/V_0 and the F_1/F_0 ratios increased as
109 contrast was reduced indicating that a change in synaptic drive is the more likely
110 explanation for the altered modulation responses of complex cells. We have
111 demonstrated that the circuitry leading to spatial phase invariant responses in
112 visual cortex depends on the strength of visual drive. This observation is
113 consistent with a scheme of complex cell generation in which the recurrent
114 inputs in the visual cortex act as amplifiers, generating linear or nonlinear
115 responses when input gain is low or high, respectively (Chance et al., 1999).
116

117 **Materials and Methods**

118 **Electrophysiology**

119 Recordings were made from anaesthetised C57BL/6 mice of both sexes
120 aged five to twelve weeks. All experiments were performed according to the
121 National Health and Medical Research Council's Australian Code of Practice for the
122 Care and Use of Animals for Scientific Purposes. All experimental procedures were
123 approved by Animal Ethics Committees of the University of Melbourne, or by the
124 Institutional Animal Care and Use Committee of the University of Texas at Austin.
125 Mice were anaesthetised with intraperitoneal injections of chlorprothixene
126 (10mg/kg) followed by Urethane (1g/kg). Animals also received an injection of
127 dexamethasone (2mg/kg) to reduce brain oedema. The level of anaesthesia was
128 monitored using the electrocardiogram (ECG) and repeated toe-pinches
129 throughout the experiment. Body temperature was monitored and maintained at
130 37°C using an auto-regulating heating blanket. A tracheotomy was performed to
131 ensure a clear airway. A craniotomy approximately 1mm × 2.5 mm was
132 performed over V1 in one hemisphere and the dura mater retracted.

133 Intracellular responses were obtained in mice via blind recordings with a
134 whole-cell configuration *in vivo* as previously described (Ferster and Jagadeesh,
135 1992; Margrie et al., 2002; Priebe et al., 2004; Tan et al., 2011). Patch pipettes
136 with tip resistances of 8–10 MΩ were pulled from borosilicate glass
137 capillaries (1.2 mm outer diameter, 0.7 mm inner diameter; KG-33, King
138 Precision Glass). A silver chloride coated silver wire was inserted into the
139 pipette, which was filled with 135 mM K-gluconate, 4 mM NaCl, 0.5 mM EGTA,
140 2 mM MgATP, 10 mM phosphocreatine disodium, and 10 mM HEPES, pH
141 adjusted to 7.3 with KOH (Sigma-Aldrich). A silver–silver chloride wire was

142 inserted as a reference electrode into muscles near the base of the skull. The
143 craniotomy as well as the reference electrode was covered with 4% agarose in
144 normal saline to keep the cortex moist and to reduce changes in the surrounding
145 fluid and concomitant changes in associated junction potentials. An Axoclamp 2B
146 patch-clamp amplifier was used in current clamp to record from neurons 150–
147 600 μm below the surface of the cortex. The voltage was digitised and recorded
148 with custom software (Labview, National Instruments), which also sent
149 instructions to a separate stimulus-generation computer.

150

151 **Visual Stimuli**

152 Visual stimuli were generated using the Psychophysics toolbox for Matlab
153 (The Mathworks Inc. Natick, MA, USA) and were presented on a calibrated CRT
154 monitor (Sony GDM-F520, 100 Hz non-interlaced refresh rate, 1280x1024 pixels,
155 25 cd/m^2 mean luminance). The viewing distance for all recordings was 30 cm.
156 For each recorded cell we measured its orientation, spatial frequency and
157 temporal frequency preferences, as well as its RF location and size using drifting
158 sinusoidal gratings. For example, to determine orientation preference, sinusoidal
159 gratings were presented at eight different orientations (0, 22.5, 45, 67.5, 90,
160 112.5, 135, 157.5°). After 0.5 s presentation of each orientation, gratings moving
161 in the opposite direction were presented and followed with 0.5 s of grey screen
162 (at the mean luminance of the prior grating). The optimal tuning parameters
163 were determined online and then applied to the experimental stimuli. The
164 contrast of the grating was defined as: Michelson contrast = $[(Lum_{\text{max}} -$
165 $Lum_{\text{min}})/Lum_{\text{max}} + Lum_{\text{min}}]] \times 100$ where Lum_{max} and Lum_{min} are the maximum
166 and minimum luminance of the grating.

167 Two types of experimental stimuli were used: drifting sinusoidal gratings
168 and sinusoidally modulated contrast-reversing gratings. Stimuli were presented
169 at the optimal temporal frequency (TF), spatial frequency (SF) and orientation of
170 the recorded cell in a circular aperture the size of its excitatory RF. Drifting
171 gratings with contrast levels ranging between 4 and 100% were presented in
172 pseudorandom order interleaved with 1 s presentations of a blank (mean
173 luminance) screen. Each grating was presented for 3 s with the first and last 0.5 s
174 stationary, and drifting for the 2 s in between. Trials were repeated as many
175 times as the stability of the recording would allow. Contrast-reversing gratings
176 were presented at 8 different spatial phases (0, 45, 90, 135, 180, 225, 270, 315°).
177 Depending on the recording stability, various combinations of contrast between
178 8 and 100% were tested. Each stimulus presentation consisted of a grating
179 presented for 0.5 s with a steady contrast, 2 s presented with sinusoidally
180 modulated contrast, and another 0.5 s with steady contrast.

181

182 **Data analysis**

183 The resting membrane potential (V_{rest}) of a patched cell, measured as the
184 responses to a blank screen (0% contrast), ranged from -40 mV to -80 mV. To
185 examine the subthreshold membrane potential modulation, spikes were
186 removed from the raw records prior to analysis using a 5 ms median filter
187 (Jagadeesh et al., 1997). The modulation ratios for membrane potential (V_1/V_0)
188 and spiking rate (F_1/F_0) to drifting gratings were calculated as previously
189 described in Priebe et al. (2004). For contrast-reversing gratings, the modulation
190 ratios for membrane potential and spiking rate were calculated as V_2/V_1 and
191 F_2/F_1 , respectively. Cycle-averaged responses were measured by aligning each

192 response cycle, excluding the first cycle. The mean and standard error of the
193 membrane potential and spiking rate were calculated at each time point of the
194 cycle-averaged response. As in Priebe et al. 2004, the mean membrane potential
195 (V_0) and spiking rate (F_0) are based on the differences between the responses
196 during a stimulus and the spontaneous responses during a blank screen of the
197 same time. Fourier coefficients at the fundamental frequency of the stimulus
198 grating (V_1 for membrane potential, F_1 for spiking rate) and at twice the stimulus
199 input (V_2 for membrane potential, F_2 for spiking rate) for each cycle-averaged
200 response were extracted using the FFT function in Matlab (The Mathworks Inc.
201 Natick, MA, USA). A perfect half-wave rectified spiking rate response is expected
202 to have an F_1/F_0 ratio of 1.57. We did find two cells with F_1/F_0 ratios above 1.57
203 at high stimulus contrasts, but this was due to low F_0 values created from
204 subtracting high spontaneous spiking rate from evoked spiking rate. All cells
205 showed significant increases in mean spiking rate (F_0) relative to the
206 spontaneous spiking rate ($p < 0.05$, one-sided t-tests). One cell with a
207 modulation ratio (F_1/F_0) of 2.67 had a relatively high spontaneous spiking rate
208 (6.9 spks/s) compared to evoked spiking rate (9.6 spks/s). The other cell with
209 F_1/F_0 of 1.98 showed a relatively high spontaneous spiking rate (1.2 spks/s)
210 compared to evoked spiking rate (6.5 spks/s). Both cells showed significant
211 increases in evoked F_1 amplitude with a clear response to the drifting grating
212 stimulus ($p = 0.0002$ and $p < 0.0001$, one-sided t-tests). Error bars were
213 generated by projecting the cycle-by-cycle estimate of modulation amplitude and
214 phase onto the mean phase and amplitude vector in complex space.

215

216 **Model**

217 Each neuron in the network model receives feedforward and recurrent input and
 218 is based on the rate model developed by Chance, Nelson and Abbott (1999). The
 219 activity of neuron i , is modelled using a simple rate model equation that includes
 220 a threshold nonlinearity:

$$221 \quad \tau_v \frac{dv_i}{dt} = I_i^{ff} + I_i^{rec} - v_i \quad (1)$$

$$222 \quad r_i = \left[\frac{v_i - v_{thresh}}{\tau_r} \right]_+ \quad (2)$$

223 where I_i^{ff} and I_i^{rec} represent the feedforward and recurrent inputs. We use a
 224 time constant, τ_r of 20 ms and a positive voltage threshold (v_{thresh}). The
 225 feedforward input is equal to a half-wave rectified sinusoidal modulation,
 226 where each network neuron has a random preferred spatial phase (ϕ_i).

$$227 \quad I_i^{ff} = \sin\left(\frac{2\pi t}{500} - \phi_i\right) \quad (3)$$

228 The recurrent input to model neuron i is given by:

$$229 \quad I_i^{rec} = \frac{1 - \phi_i}{N} r_i \quad (4)$$

230 The degree of recurrent and feedforward input is set by the value of ϕ_i , which
 231 was randomly set between 0 and 1, with zero reflecting all recurrent input and
 232 one reflecting all feedforward input.

233

234 **Results**

235 We first explored a model of the transformation between simple and
236 complex cells to guide our experiments based on the architecture from Chance et
237 al. (1999). They used a rate model to demonstrate that the degree of simple cell
238 and complex cell behaviour is related to the amount of recurrent circuitry in the
239 network. We implemented their model with two changes. First, each neuron
240 received a random degree of feedforward input ($\frac{w_i}{\sigma_i}$) so that we would observe
241 both simple and complex cells within the same network. Second, we included a
242 non-zero threshold to model the threshold nonlinearity between the input and
243 output. Both simple and complex cells emerge from this network model, as seen
244 in the modulation ratio to a drifting grating (Fig. 1A). Simple cells respond at one
245 phase of the stimulus and have a modulation ratio that is greater than 1 (Fig. 1A,
246 top row). Network complex cells exhibit a response that varies little with the
247 drifting grating and are characterized by a modulation ratio less than 1 (Fig. 1A,
248 bottom row). Importantly in this network simulation we can view neurons that
249 exhibit combinations of linear and nonlinear components (Fig 1A, middle row)
250 and therefore have a modulation ratio between 0.5 and 1.

251 As the emergence of complex cells in this model depends on the degree of
252 recurrent amplification, we hypothesized that reducing the input strength would
253 impact the modulation ratios of network neurons, and thus the degree of
254 generalization across spatial phase. Indeed, we find that reducing input strength,
255 or visual contrast, leads to systematic increases in the modulation ratios of
256 network neurons (Fig. 1B). The modulation ratios of model neurons shift to
257 higher values as the input strength is reduced, even switching neurons that

258 would be classified as complex for high contrast to being simple at low contrast
259 (Fig. 1A, middle row). Contrast-dependent changes in the modulation ratio could
260 therefore reflect the amplification structure of the model visual cortex. There are
261 two components that contribute to the increase in modulation ratio with
262 contrast. First, the observed increase in the network modulation ratio with
263 contrast depends on the voltage threshold (V_{thresh}). If the voltage threshold is set
264 to 0 then no change in modulation ratio occurs with changes in contrast (data
265 not shown). Second, there are systematic increases in the synaptic modulation
266 ratio (Fig. 1C) as contrast is reduced. This simple model demonstrates how the
267 cortical circuitry, acting as an amplifier, could generate spatially invariant
268 responses and demonstrates that the degree of the spatial invariance depends on
269 the input strength.

270 There are other possible models that could explain the shift in modulation
271 ratio due to changes in contrast. One alternative possibility is an “iceberg” effect
272 where not all synaptic responses are converted into spiking activities (Carandini
273 and Ferster, 2000; Mechler and Ringach, 2002; Priebe et al., 2004). For a high
274 contrast stimulus, the synaptic input is sufficient to evoke spiking responses at
275 all phases (Hietanen et al. 2013), whereas for a low contrast stimulus, the
276 synaptic input falls below threshold and is only sufficient to evoke spiking
277 responses for a subset of phases (Fig. 2A). In this model, the modulation ratio
278 of the synaptic input (V_1/V_0 : the modulation ratio of the membrane
279 potential) does not vary (Fig. 2B); instead the change in the spiking modulation
280 ratio is due to the threshold nonlinearity. This explanation for the observed
281 changes in the spike modulation ratio with contrast proposes that the underlying

282 membrane potential modulation ratio is fixed and the changes observed at the
283 level of spiking emerge from the threshold nonlinearity.

284 To examine whether signatures of these models exist in V1 neuron
285 responses we measured the degree to which the modulation ratio of the synaptic
286 input varies with contrast. Previous experimental reports have demonstrated
287 that the spiking modulation ratio of V1 neurons is contrast dependent, which
288 matches the pattern shown in the model, i.e. responses become more simple-like
289 as contrast declines. However, these records do not differentiate between
290 synaptic changes from the network and changes that may exclusively emerge
291 from threshold nonlinearity. To determine whether the change in the spiking
292 modulation ratio is due to threshold or synaptic mechanisms, we recorded
293 intracellularly from V1, giving us access to both the underlying membrane
294 potential as well as the spiking rate in response to gratings. We recorded from
295 20 cells with drifting gratings and 21 cells with contrast reversing gratings in 20
296 urethane-anaesthetised mice.

297

298 **Responses to drifting gratings**

299 Based on responses to drifting sinusoidal gratings, mouse V1 neurons
300 show the same separation into simple and complex cells as cats and primates
301 (Niell and Stryker, 2008). We classified cells as simple by the large modulation of
302 spiking rate ($F_1/F_0 > 1$) to a drifting grating stimulus. The underlying membrane
303 potential of these neurons also exhibited large modulations when stimulated at
304 the preferred orientation, spatial frequency and temporal frequency (Fig. 3,
305 100% contrast). Membrane potential fluctuations were separated from spiking
306 rate by identifying the spike times and removing them from the membrane

307 potential traces using a median filter (see Methods). Both the raw response and
308 the trial-averaged membrane potential for the simple cell in Figure 3 are highly
309 modulated at the input frequency and phase-locked to the sinusoidal grating
310 stimulus (Fig. 3, bottom).

311 Previous work has demonstrated that the classification of simple cells
312 does not vary with contrast in the cat and primate (cat: Crowder et al., 2007; van
313 Kleef et al., 2010; monkey: Henry and Hawken, 2013; Cloherty and Ibbotson,
314 2015; Meffin et al., 2015). We first examined whether this is also true in mouse
315 V1 by measuring the changes in the modulation ratios for spiking rate (F_1/F_0)
316 and membrane potential (V_1/V_0) of individual simple cells with contrast (Fig.
317 4A). For simple cells, V_1/V_0 did vary with contrast but the F_1/F_0 was consistently
318 higher than unity, indicating that simple cell classification does not depend on
319 contrast (Fig. 4A). Across our sample population we found that the subthreshold
320 modulation ratio (V_1/V_0) of simple cells often increased with decreasing contrast
321 but this change was not statistically significant ($n = 13$, $p > 0.05$, one-sided t-test;
322 red symbols in Fig. 5A). This result is consistent with results from an earlier
323 study, in which simple cells in cat V1 showed increased V_0 and V_1 as contrasts
324 decreased (Carandini and Ferster, 1997). Despite those subthreshold changes,
325 however, the F_1/F_0 ratio was consistently above unity for simple cells at low and
326 high contrasts (Fig. 5B). Therefore, the simple cell population remains highly
327 phase sensitive at both the membrane potential and spiking output levels for all
328 contrasts.

329 We next examined how contrast alters the modulation ratio of complex
330 cells in mouse V1. As found in other mammals, complex cells modulate more at
331 low contrasts than high contrasts (cat: Crowder et al., 2007; van Kleef et al.,

332 2010; monkey: Henry and Hawken, 2013; Cloherty and Ibbotson, 2015; Meffin et
333 al., 2015). We found a range of contrast-dependent shifts in the modulation
334 ratios, which demonstrate that synaptic mechanisms are involved in this
335 process. For some complex cells modulations in response amplitude are clearly
336 evoked across all contrasts at the level of both the membrane potential and
337 spiking rate (Fig. 4B). Measures of the modulation ratios of the membrane
338 potentials systematically increase as contrast decreases. This shift is matched by
339 a commensurate increase in the F_1/F_0 ratios. For both spiking rate and
340 membrane potential responses, the mean responses (F_0 & V_0) dominate the
341 modulation amplitudes (F_1 & V_1) at high contrasts (Fig. 4B). As the contrast
342 decreases, however, the differences between these two parameters declines and
343 results in increased modulation ratios. This trend is especially prominent in the
344 membrane potential responses in which V_1 remains largely unchanged compared
345 to V_0 . When considering the complex cell and the simple cell examples together,
346 it is noticeable that similar membrane potential characteristics in the two
347 example cells (Fig. 4A & B) are observed at higher contrasts (32% and 64%).
348 Both cells show substantial modulations of the fundamental frequencies of the
349 input (V_1) that are well above the resting membrane potential, which result in
350 the V_0 component being larger than the V_1 component. However, the spiking
351 responses show different response characteristics in the two cells: cell A has a
352 larger F_1 component at high contrasts whereas cell B has a larger F_0 component
353 (Fig. 4A & 4B). As a result, cell A has an $F_1/F_0 > 1$ and is therefore classified as a
354 simple cell, whereas Cell B is classified as a complex cell because it has an $F_1/F_0 <$
355 1. These observations suggest that the dichotomy between simple and complex
356 cells based on spiking modulation ratios with high stimulus strengths does not

357 directly translate to corresponding distinctions in the membrane potential
358 responses. The differences in the F_1/F_0 ratios in the two cells are likely the result
359 of non-linear threshold transformations from the membrane potentials to the
360 spiking outputs (Priebe et al., 2004).

361 At the population level, changes in the F_1/F_0 (spiking rate) and V_1/V_0
362 (membrane potential) ratios of complex cells at high and low contrasts have
363 characteristics similar to the responses of the synaptic model. The scatter plots
364 of both F_1/F_0 and V_1/V_0 show significant increases at low contrast compared to
365 high contrast (Fig. 5). The distribution of V_1/V_0 ratios presented as a histogram
366 reveal a significant shift towards higher values at low contrasts compared to
367 high contrasts ($n = 20$, $p = 0.008$, one-sided t-test; blue symbols in Fig. 5A). The
368 population spiking responses also show significant increases in F_1/F_0 ratios at
369 low contrasts ($n = 20$, $p = 0.02$, one-sided t-test, Fig. 5B).

370

371 **Responses to contrast reversing gratings**

372 An alternative method to quantify the nonlinearities of cortical neurons is
373 to examine the modulated responses to contrast-reversing gratings (Hawken and
374 Parker, 1987). An ideal simple cell should modulate at the temporal frequency of
375 the contrast reversal (F_1), and the timing of its response should depend on the
376 spatial phase of the grating (Fig. 6, left). An ideal complex cell should modulate
377 at twice the temporal frequency of the contrast reversal (F_2), and the timing of its
378 response should not depend on the spatial phase of the grating (Fig. 6, right).
379 One can then distinguish simple and complex cells by considering the first and
380 second Fourier components in the complex plane (Fig. 6B). Simple cells should
381 have large F_1 components that lie along an axis in the complex plane. For the

382 example simple cell, that axis is along the abscissa. In contrast, the example
383 complex cell has small F_1 components, but a large F_2 component for which the
384 response does not change with the stimulus phase. To extract a metric that
385 describes the relative F_1 and F_2 modulations of the responses, we computed the
386 amplitude of the projection of the F_1 values onto their principle axis in the
387 complex plane, and compared that to the vector average F_2 value in the complex
388 plane. Doing so enforces the expectation that the timing of the F_2 component
389 should be invariant to spatial phase. The resulting contrast reversing modulation
390 index (F_2/F_1) is large for complex cells and small for simple cells.

391 To quantify how much V1 neurons shift to more simple-like behaviour as
392 contrast is lowered, we presented contrast-reversing gratings at eight different
393 spatial phases and extracted the phase and amplitude of the Fourier components
394 at the temporal frequency of the reversing gratings and at twice the temporal
395 frequency of the reversing gratings (Fig. 7). These measurements were made
396 both for the spiking rate of the neurons and their underlying membrane
397 potentials.

398 As with drifting gratings we found that reductions in contrast caused
399 systematic changes in membrane potential modulations that reflected a shift
400 toward more simple-like behaviour in complex cells. At high contrast these
401 complex cells are characterized by frequency doubled responses in both
402 membrane potential and spiking rate (Fig. 7A). When contrast was lowered,
403 however, the amplitude of the frequency doubled responses declined relative to
404 the modulation at the temporal frequency of the reversing grating. Note that not
405 only do modulations emerge at low contrasts, but the timing of the modulations

406 systematically shifts with the spatial phases of the gratings, as predicted by an
407 ideal simple cell (Fig. 6).

408 As shown in the membrane potential and spiking rate traces, the
409 projected F_2 and F_1 modulations vary across stimulus phase (Fig. 7B). To
410 quantify the changes outlined above for each cell, we estimated individual F_1 &
411 F_2 (spikes) and V_1 & V_2 (membrane potentials) values across all spatial phases
412 for each stimulus contrast tested. For F_2 and V_2 , we simply averaged across all
413 stimulus spatial phases since these values were spatial phase-invariant (red lines
414 in Fig. 6C and Fig. 7B). However, averaging across all stimulus spatial phases
415 does not work for F_1 and V_1 because they are spatial phase dependent (blue lines
416 in Fig. 6C and Fig. 7B). At high contrasts the amplitudes of the F_2 and V_2
417 modulations do not modulate with spatial phase, while the F_1 and V_1 components
418 clearly modulate. When contrast is lowered, the F_2 and V_2 modulation
419 amplitudes decline more rapidly relative to the F_1 and V_1 components,
420 respectively. These changes cause an overall decline in the membrane potential
421 modulation ratio (V_2/V_1) from 0.7 at high contrast to 0.12 at low contrast (Fig.
422 8A, arrow). As small modulation ratios are associated with simple cells and
423 larger ones with complex cells, this is an example in which contrast shifts the
424 behaviour of the neuron toward more simple-like responses.

425 To quantify how contrast altered the behaviour of our complex cell
426 population we estimated V_2/V_1 and F_2/F_1 modulation indices across our sample
427 population (membrane potential: $n = 21$, spikes: $n = 12$; Fig. 8). We found that
428 the membrane potential modulation ratio systematically declined with contrast,
429 changing from a mean value of 0.83 to 0.57 ($P = 0.016$, one-sided t-test). There
430 was a similar, but more modest, change in the modulation ratios obtained from

431 spiking rate across our sample population ($P = 0.021$, one-sided t-test).

432 Therefore, as with drifting gratings, neurons in mouse visual cortex shift toward

433 more simple-like responses as contrast is lowered.

434

435 **Discussion**

436 Contrast-dependent phase sensitivity has been documented in a
437 subpopulation of neurons in the primary visual cortex of cat (Crowder et al.,
438 2007; van Kleef et al., 2010; Hietanen et al., 2013) and primate (Henry and
439 Hawken, 2013; Cloherty and Ibbotson, 2015). The current study demonstrates
440 that contrast-dependent phase sensitivity is also present in the primary visual
441 cortex of mouse. Cortical visual processing in mice has been studied extensively
442 in the past decade (Niell and Stryker, 2008; Huberman and Niell, 2011; Tan et al.,
443 2011). The abundant opportunities for genetic manipulation have made mouse
444 visual cortex a useful model in addition to carnivores and primates for studying
445 RF properties (e.g. Wang et al., 2006; Liu et al., 2009; Zariwala et al., 2011). All
446 previous literature showing contrast-dependent changes in response linearity in
447 cats and monkeys has been quantified using modulation ratios calculated from
448 extracellular responses to drifting sinusoidal gratings (Crowder et al., 2007; van
449 Kleef et al., 2010; Henry and Hawken, 2013; Hietanen et al., 2013; Cloherty and
450 Ibbotson, 2015) or contrast-reversing gratings (Meffin et al., 2015).

451 We used whole cell recordings to shed light on how complex cells emerge
452 in V1. A simple model to describe this process is that recurrent cortical
453 connectivity between neurons with distinct spatial selectivity generates the
454 spatial-invariant responses that characterize complex cells. Two models have
455 been proposed to describe this shift, one from Hubel and Wiesel in which simple
456 cells receive inputs from the dorsal lateral geniculate nucleus (dLGN) in the
457 thalamus and converge onto complex cells in one step to generate spatial
458 invariance (Hubel and Wiesel, 1962). Alternatively the generation of spatial
459 invariance may require many steps, which reflect an increase in the proportion

460 of cortical circuitry that neurons receive (Chance et al., 1999). One way to
461 distinguish these possibilities is to observe how input strength alters the
462 emergence of complex cells. Mouse LGN neurons show mostly linear contrast
463 sensitivity, the responses of individual LGN cells increase with increasing
464 contrasts (Grubb and Thompson, 2003; Tang et al., 2016). Lien and Scanziani
465 (2013) have shown that recurrent cortical excitation to simple cells in mouse V1
466 are phase-sensitive and matches their LGN inputs. However, it is unclear if this is
467 the case for complex cells. We demonstrate that as contrast declines both
468 membrane potential and spiking modulation ratios increase, as expected from
469 the recurrent model proposed by Chance et al. (1999).

470 An alternative explanation for the shift in modulation ratio at low contrast
471 is the variability of contrast response curves across simple cells. Neurons within
472 V1 vary in the contrast at which they saturate, such that for some neurons the
473 changes in contrast may yield large changes in response amplitude whereas for
474 others they may evoke little effect (Van den Bergh et al. 2010). A simple model
475 that includes the variance in the contrast response curves of simple cells which
476 converge onto a complex could only account for input modulation ratio shifts of
477 less than 0.1, relative to our measures of modulation ratio shifts of more than
478 0.45 (data not shown).

479 We analysed the responses to drifting gratings and found that there is a
480 shift in the input modulation ratio (V_1/V_0) with contrast consistent with a
481 synaptic model (mean V_1/V_0 high contrast: 0.62, low contrast: 1.09). While the
482 threshold nonlinearity may play a role in altering the phase sensitivity of
483 neurons (Priebe et al., 2004), there is a clear synaptic component to the shift in
484 phase sensitivity. Also, as expected, when stimulated with high-contrast

485 reversing gratings these cells exhibited various degrees of frequency-doubled
486 responses (Meffin et al., 2015). However, at low contrasts, the same cells showed
487 more modulated, phase sensitive responses to drifting gratings and a tendency
488 to respond to selected spatial phases during stimulation with contrast-reversing
489 gratings.

490 In summary, for some years now it has been noted that complex cells
491 show increased modulatory responses at low contrasts, suggesting that they are
492 more phase sensitive at low contrasts (Crowder et al., 2007; van Kleef et al.,
493 2010; Henry and Hawken, 2013; Cloherty and Ibbotson, 2015; Meffin et al.,
494 2015). We demonstrate that this is not simply a manifestation of the ‘iceberg’
495 phenomenon (Carandini and Ferster, 2000; Mechler and Ringach, 2002; Priebe
496 et al., 2004), but instead a systematic shift in the inputs that cortical neurons
497 receive. This network level change in input modulation with contrast is
498 consistent with a model for the generation of invariant responses in which
499 complex cells emerge steadily through the cortical network through increases in
500 the degree of recurrent inputs that they receive.

501 **References**

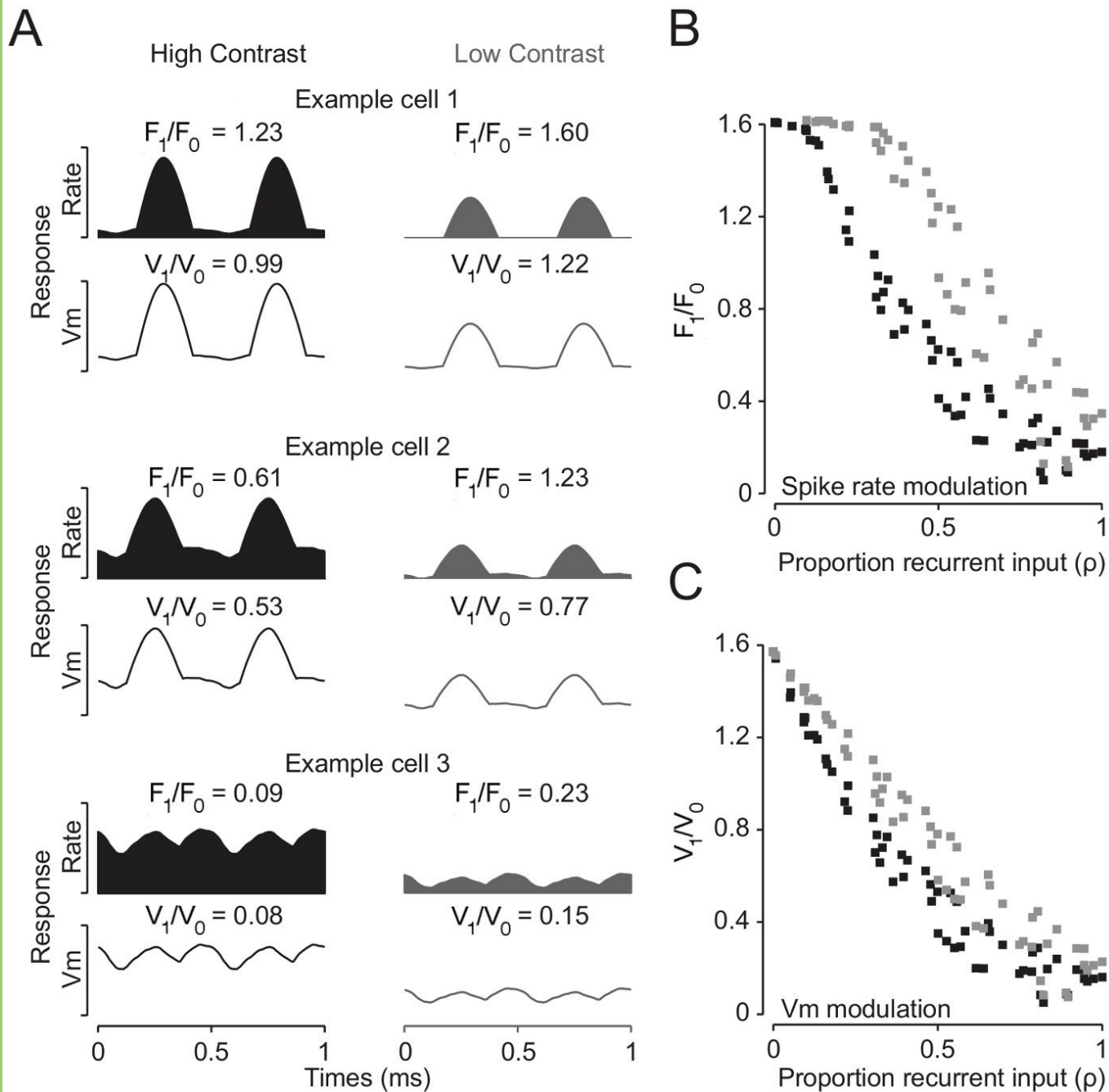
- 502 Adelson EH, Bergen JR (1985) Spatiotemporal Energy Models for the Perception
503 of Motion. *J Opt Soc Am A* 2:284-299.
- 504 Benyishai R, Baror RL, Sompolinsky H (1995) Theory of Orientation Tuning in
505 Visual-Cortex. *P Natl Acad Sci USA* 92:3844-3848.
- 506 Carandini M, Ferster D (1997) A tonic hyperpolarization underlying contrast
507 adaptation in cat visual cortex. *Science* 276:949-952.
- 508 Carandini M, Ferster D (2000) Membrane potential and firing rate in cat primary
509 visual cortex. *The Journal of neuroscience : the official journal of the*
510 *Society for Neuroscience* 20:470-484.
- 511 Chance FS, Nelson SB, Abbott LF (1999) Complex cells as cortically amplified
512 simple cells. *Nat Neurosci* 2:277-282.
- 513 Cloherty SL, Ibbotson MR (2015) Contrast-dependent phase sensitivity in V1 but
514 not V2 of macaque visual cortex. *J Neurophysiol* 113:434-444.
- 515 Crowder NA, van Kleef J, Dreher B, Ibbotson MR (2007) Complex cells increase
516 their phase sensitivity at low contrasts and following adaptation. *J*
517 *Neurophysiol* 98:1155-1166.
- 518 De Valois RL, Albrecht DG, Thorell LG (1982) Spatial frequency selectivity of cells
519 in macaque visual cortex. *Vision research* 22:545-559.
- 520 Douglas RJ, Koch C, Mahowald M, Martin KAC, Suarez HH (1995) Recurrent
521 Excitation in Neocortical Circuits. *Science* 269:981-985.
- 522 Ferster D, Jagadeesh B (1992) EPSP-IPSP interactions in cat visual cortex studied
523 with in vivo whole-cell patch recording. *J Neurosci* 12:1262-1274.
- 524 Gilbert CD (1977) Laminar Differences in Receptive-Field Properties of Cells in
525 Cat Primary Visual-Cortex. *J Physiol-London* 268:391-421.

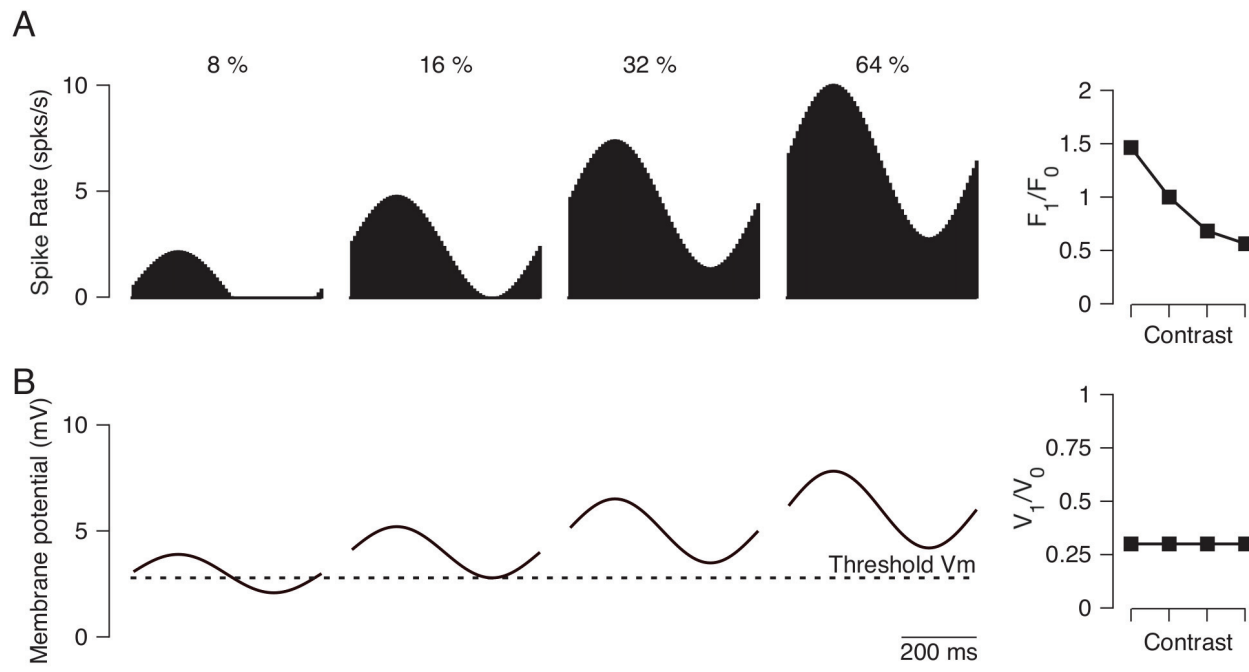
- 526 Grubb MS, Thompson ID (2003) Quantitative characterization of visual response
527 properties in the mouse dorsal lateral geniculate nucleus. *J Neurophysiol*
528 90:3594-3607.
- 529 Hammond P, Ahmed B (1985) Length Summation of Complex Cells in Cat Striate
530 Cortex - a Reappraisal of the Special Standard Classification. *Neuroscience*
531 15:639-649.
- 532 Hawken MJ, Parker AJ (1987) Spatial Properties of Neurons in the Monkey
533 Striate Cortex. *Proc R Soc Ser B-Bio* 231:251-288.
- 534 Henry CA, Hawken MJ (2013) Stability of simple/complex classification with
535 contrast and extraclassical receptive field modulation in macaque V1. *J*
536 *Neurophysiol* 109:1793-1803.
- 537 Henry GH (1977) Receptive-Field Classes of Cells in Striate Cortex of Cat. *Brain*
538 Res 133:1-28.
- 539 Hietanen MA, Cloherty SL, van Kleef JP, Wang C, Dreher B, Ibbotson MR (2013)
540 Phase Sensitivity of Complex Cells in Primary Visual Cortex. *Neuroscience*
541 237:19-28.
- 542 Hubel DH, Wiesel TN (1962) Receptive fields, binocular interaction and
543 functional architecture in the cat's visual cortex. *The Journal of physiology*
544 160:106-154.
- 545 Huberman AD, Niell CM (2011) What can mice tell us about how vision works?
546 *Trends Neurosci* 34:464-473.
- 547 Jagadeesh B, Wheat HS, Kontsevich LL, Tyler CW, Ferster D (1997) Direction
548 selectivity of synaptic potentials in simple cells of the cat visual cortex. *J*
549 *Neurophysiol* 78:2772-2789.

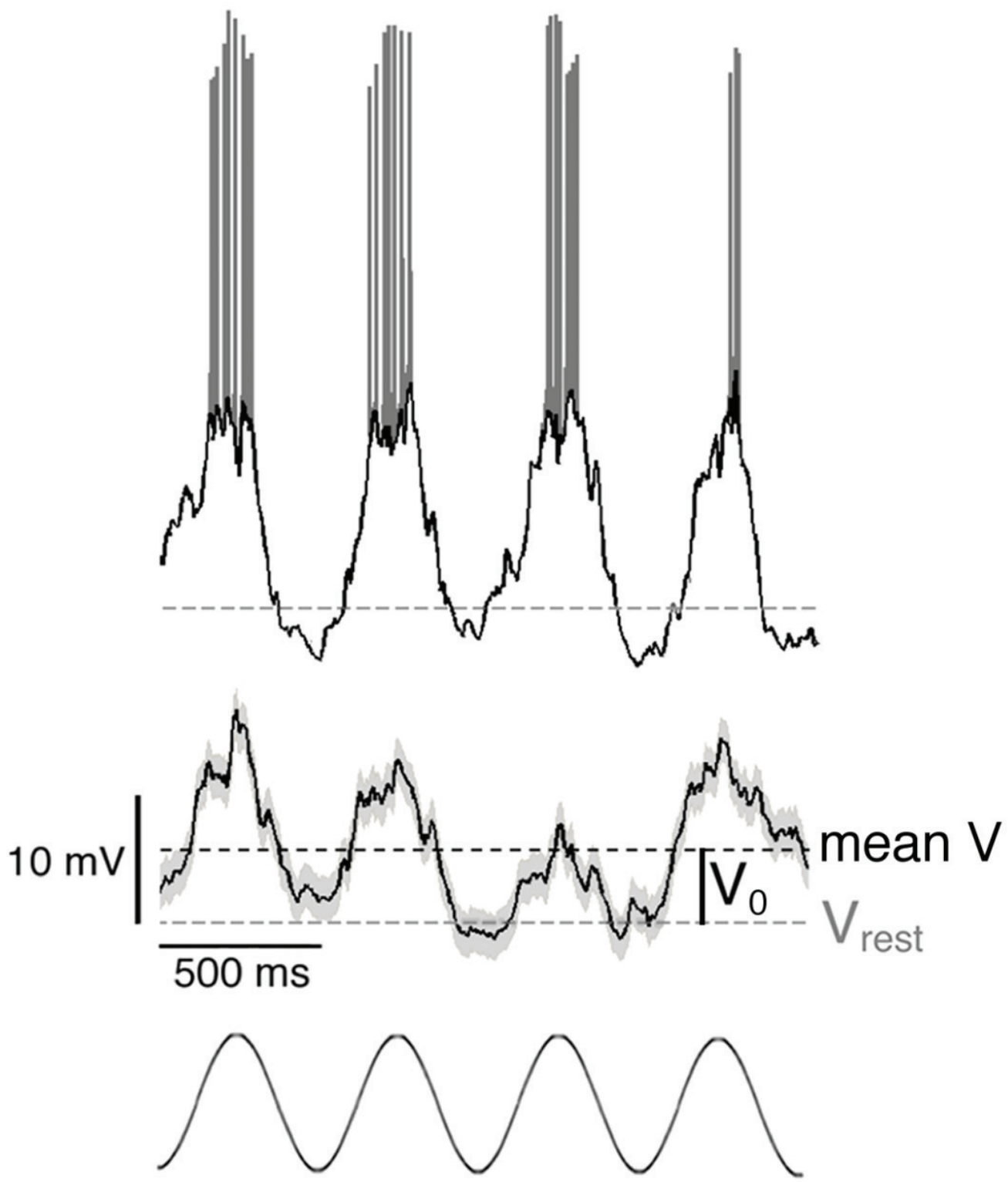
- 550 Lien AD, Scanziani M (2013) Tuned thalamic excitation is amplified by visual
551 cortical circuits. *Nature Neuroscience* 16:1315-U1207.
- 552 Liu BH, Li P, Li YT, Sun YJ, Yanagawa Y, Obata K, Zhang LI, Tao HW (2009) Visual
553 receptive field structure of cortical inhibitory neurons revealed by two-
554 photon imaging guided recording. *J Neurosci* 29:10520-10532.
- 555 Maffei L, Fiorenti A (1973) Visual-Cortex as a Spatial Frequency Analyzer. *Vision*
556 *Research* 13:1255-1267.
- 557 Margrie TW, Brecht M, Sakmann B (2002) In vivo, low-resistance, whole-cell
558 recordings from neurons in the anaesthetized and awake mammalian
559 brain. *Pflugers Arch* 444:491-498.
- 560 Martinez LM, Wang Q, Reid RC, Pillai C, Alonso JM, Sommer FT, Hirsch JA (2005)
561 Receptive field structure varies with layer in the primary visual cortex.
562 *Nature neuroscience* 8:372-379.
- 563 Mechler F, Ringach DL (2002) On the classification of simple and complex cells.
564 *Vision Res* 42:1017-1033.
- 565 Meffin H, Hietanen MA, Cloherty SL, Ibbotson MR (2015) Spatial phase sensitivity
566 of complex cells in primary visual cortex depends on stimulus contrast. *J*
567 *Neurophysiol* 114:3326-3338.
- 568 Movshon JA, Thompson ID, Tolhurst DJ (1978) Spatial and Temporal Contrast
569 Sensitivity of Neurons in Areas-17 and Areas-18 of Cats Visual-Cortex. *J*
570 *Physiol-London* 283:101-120.
- 571 Niell CM, Stryker MP (2008) Highly selective receptive fields in mouse visual
572 cortex. *J Neurosci* 28:7520-7536.

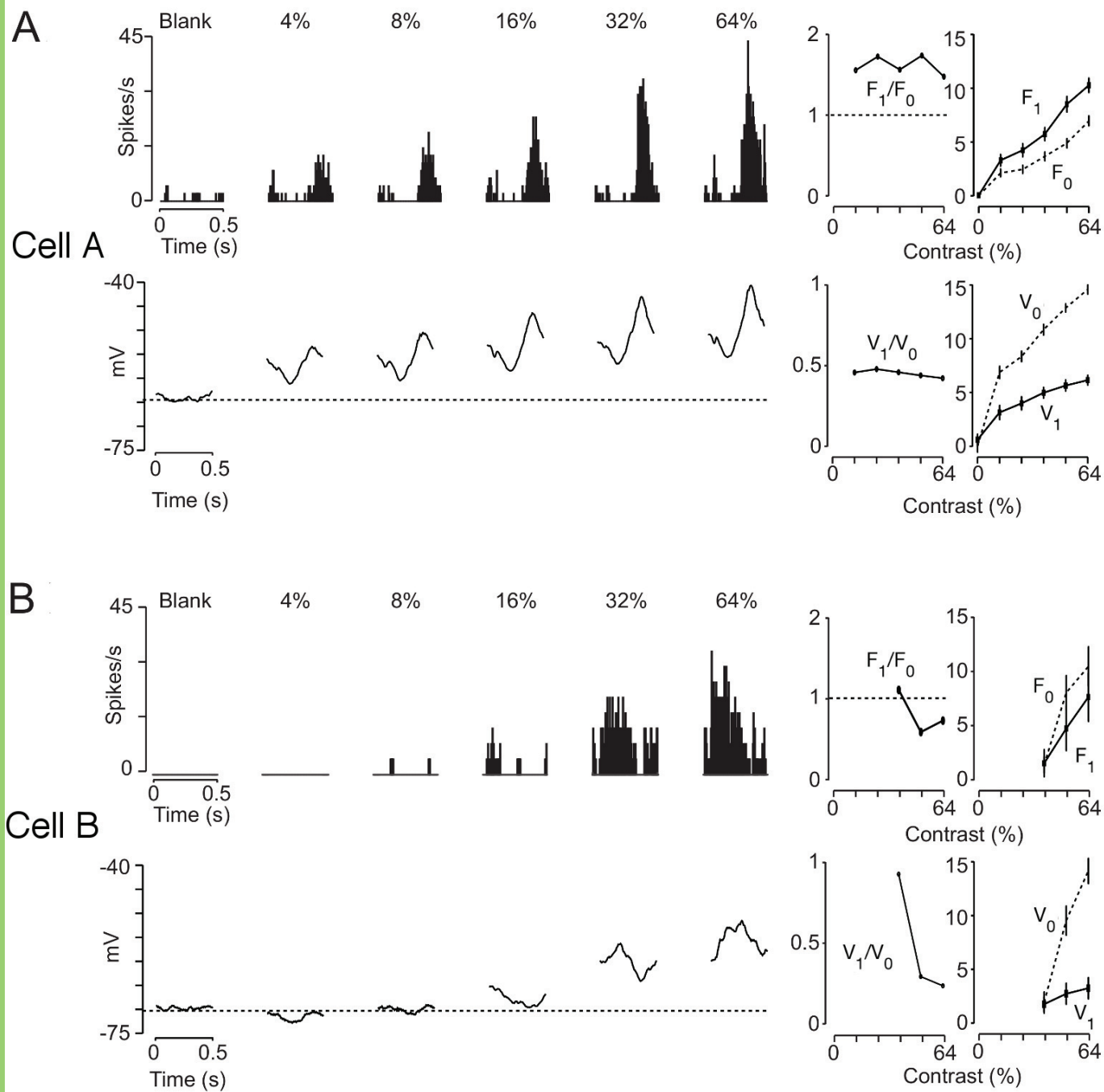
- 573 Priebe NJ, Mechler F, Carandini M, Ferster D (2004) The contribution of
574 threshold to the dichotomy of cortical simple and complex cells. *Nat*
575 *Neurosci* 7:1113-1122.
- 576 Ringach DL, Shapley RM, Hawken MJ (2002) Orientation selectivity in macaque
577 V1: Diversity and Laminar dependence. *Journal of Neuroscience* 22:5639-
578 5651.
- 579 Skottun BC, De Valois RL, Grosf DH, Movshon JA, Albrecht DG, Bonds AB (1991)
580 Classifying simple and complex cells on the basis of response modulation.
581 *Vision research* 31:1079-1086.
- 582 Somers DC, Nelson SB, Sur M (1995) An Emergent Model of Orientation
583 Selectivity in Cat Visual Cortical Simple Cells. *Journal of Neuroscience*
584 15:5448-5465.
- 585 Spitzer H, Hochstein S (1988) Complex-Cell Receptive-Field Models. *Prog*
586 *Neurobiol* 31:285-309.
- 587 Tan AY, Brown BD, Scholl B, Mohanty D, Priebe NJ (2011) Orientation selectivity
588 of synaptic input to neurons in mouse and cat primary visual cortex. *J*
589 *Neurosci* 31:12339-12350.
- 590 Tang JY, Jimenez SCA, Chakraborty S, Schultz SR (2016) Visual Receptive Field
591 Properties of Neurons in the Mouse Lateral Geniculate Nucleus. *Plos One*
592 11.
- 593 Van den Bergh Gert, Zhang Bin, Arckens Lutgarde, Chino YM (2010) Receptive
594 field properties of V1 and V2 neurons in mice and macaque monkeys. *J*
595 *Comp Neurol* 518:2051-2070
- 596 van Kleef JP, Cloherty SL, Ibbotson MR (2010) Complex cell receptive fields:
597 evidence for a hierarchical mechanism. *J Physiol* 588:3457-3470.

- 598 Wang KH, Majewska A, Schummers J, Farley B, Hu C, Sur M, Tonegawa S (2006)
599 In vivo two-photon imaging reveals a role of arc in enhancing orientation
600 specificity in visual cortex. *Cell* 126:389-402.
- 601 Williams PE, Shapley RM (2007) A dynamic nonlinearity and spatial phase
602 specificity in macaque V1 neurons. *J Neurosci* 27:5706-5718.
- 603 Zariwala HA, Madisen L, Ahrens KF, Bernard A, Lein ES, Jones AR, Zeng H (2011)
604 Visual tuning properties of genetically identified layer 2/3 neuronal types
605 in the primary visual cortex of cre-transgenic mice. *Front Syst Neurosci*
606 4:162.
607

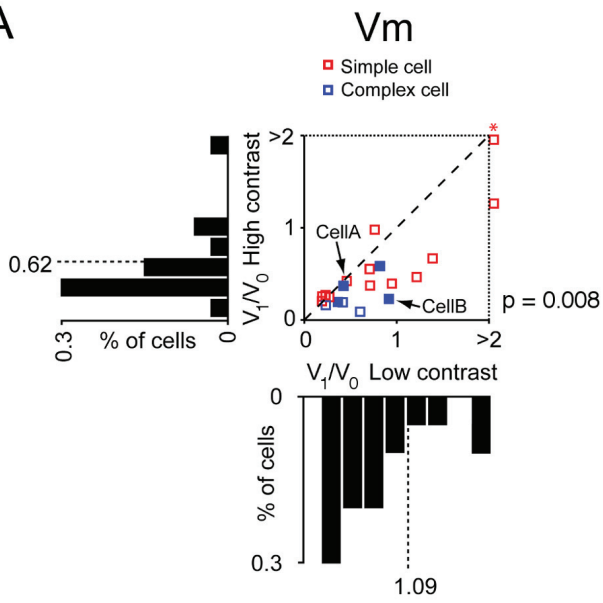




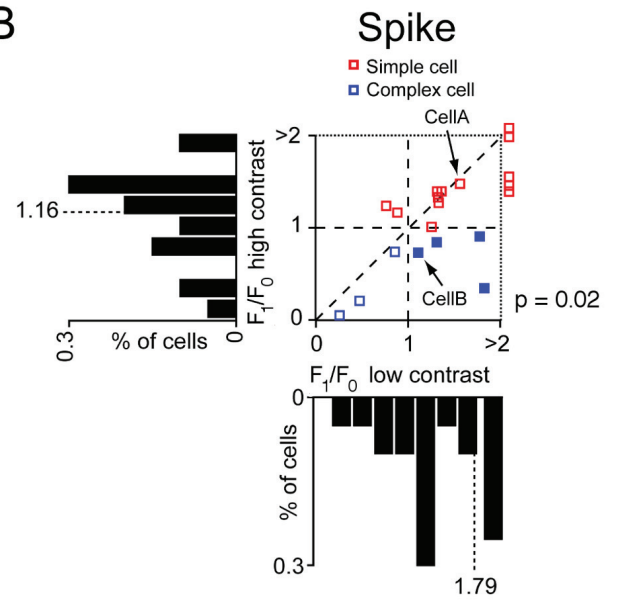


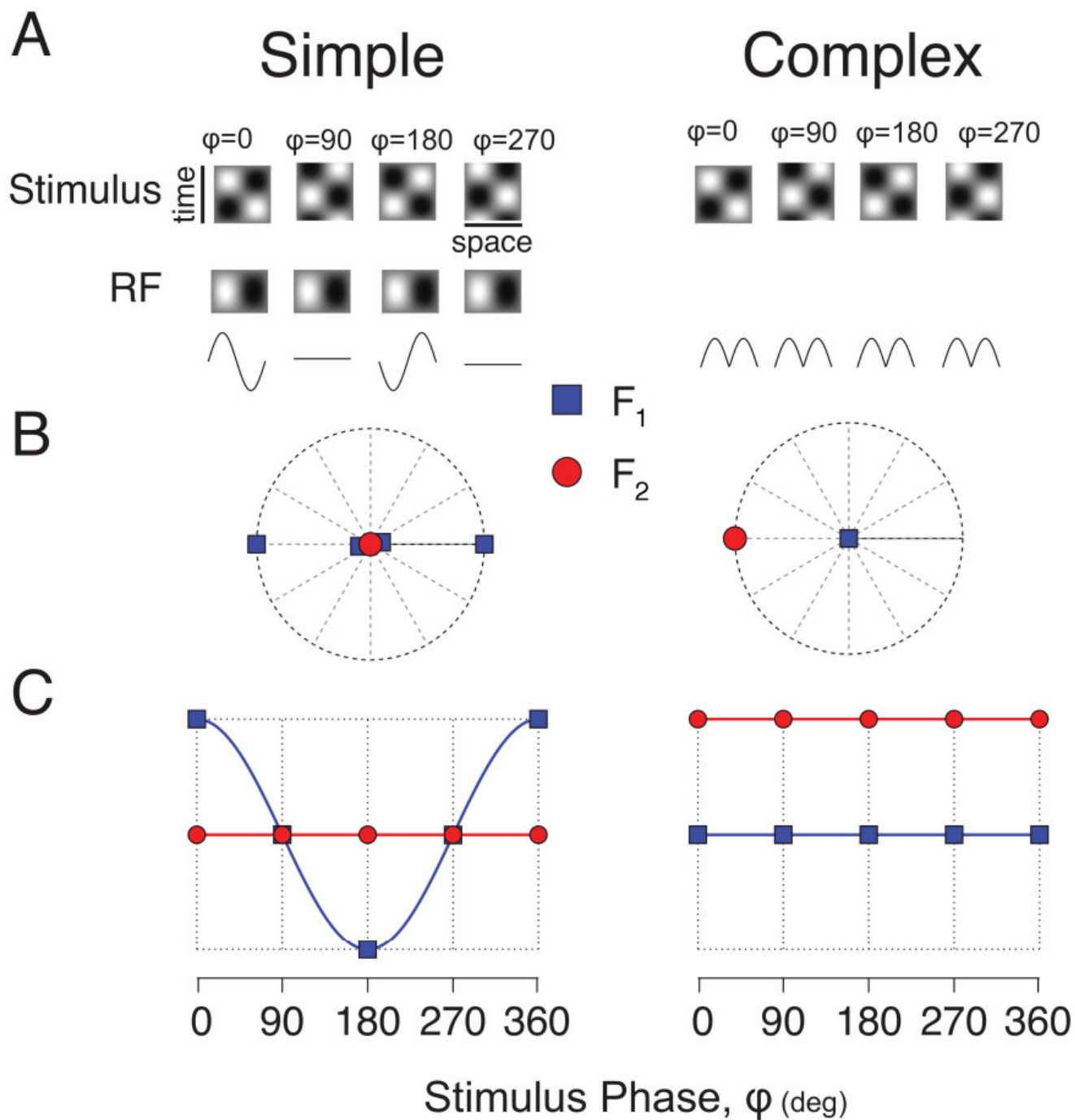


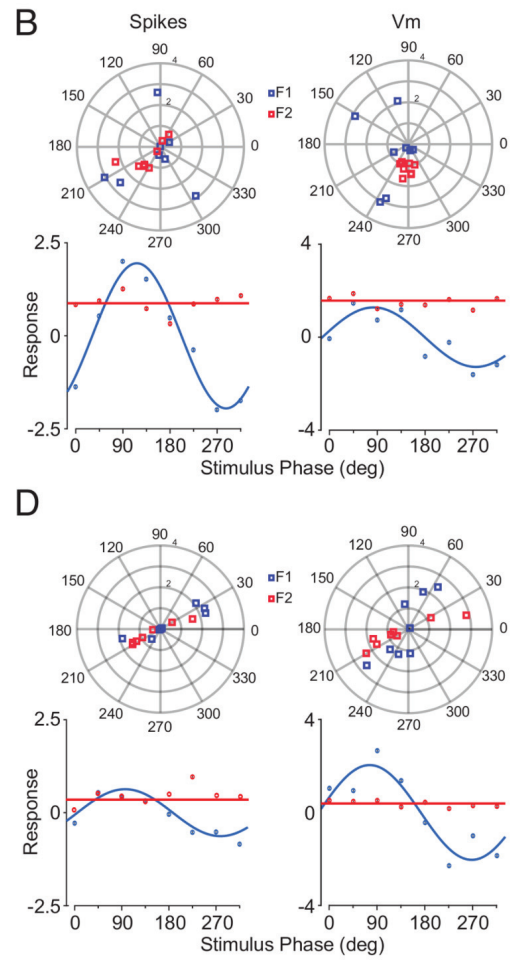
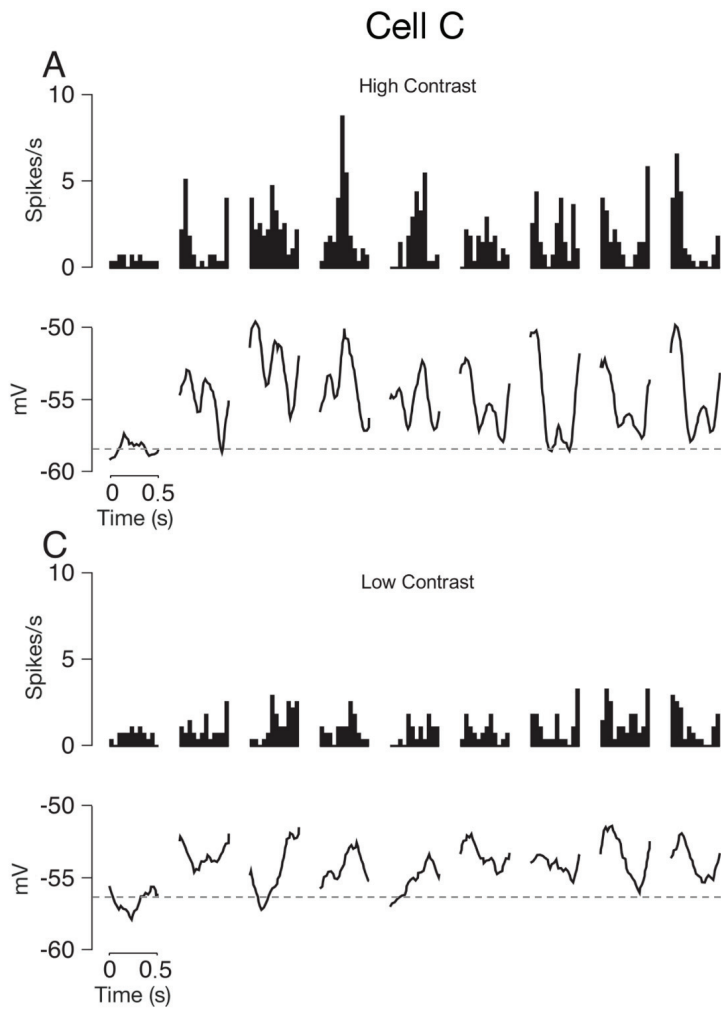
A



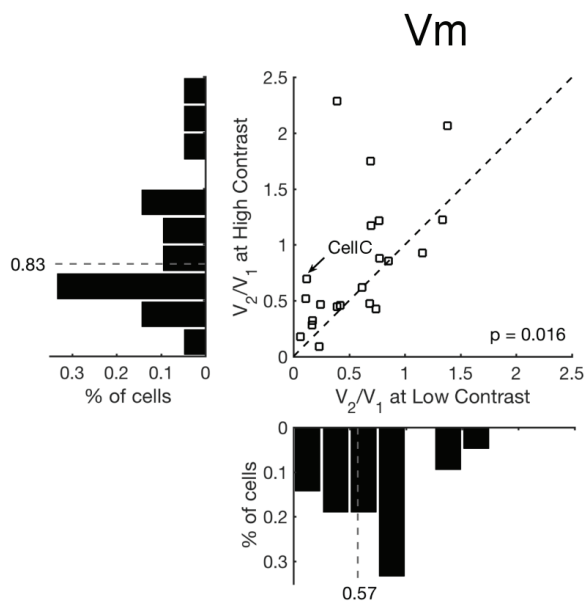
B







A



B

